



A complete residual stress model for laser surface hardening of complex medium carbon steel components



Erica Liverani, Adrian H.A. Lutey^{*}, Alessandro Ascari, Alessandro Fortunato, Luca Tomesani

Università di Bologna, Dipartimento di Ingegneria Industriale (DIN), viale Risorgimento, 2, Bologna, Italy

ARTICLE INFO

Article history:

Received 7 March 2016

Revised 5 May 2016

Accepted in revised form 22 May 2016

Available online 26 May 2016

Keywords:

Laser hardening

Residual stress

COMSOL multiphysics

X-ray diffraction

ABSTRACT

A numerical model is presented for evaluation of residual stresses following laser surface treatment of mechanical components with arbitrary geometry. Following on from previous temperature and microstructural models, stress evaluation is performed by considering the resulting deformation from thermal expansion, elastic and plastic deformation, and microstructural changes. A 3.3 kW diode laser with wavelength of 930 nm and 34 mm × 2 mm rectangular spot is utilized to perform heat treatment experiments on an AISI 9810 steel cam, with x-ray diffraction measurements performed before and after laser exposure to determine circumferential and axial surface stresses. Verification of model accuracy is performed by comparing calculated stresses with the measured values. The influence of incident laser fluence and scanning velocity on the hardened depth and residual stress state is then investigated numerically for the same component. It is found that higher laser fluence, or an increase in exposure velocity at constant fluence, leads to an increase in the hardened depth and a reduction in compressive residual stresses.

© 2016 Elsevier B.V. All rights reserved.

1. Introduction

Laser surface hardening of hypo-eutectoid steels presents a number of advantages over traditional flame and induction surface hardening, including lack of a quenching medium, low distortion, high hardness and selective treatment [1]. The process yields improved flexibility due to the highly localized nature of laser irradiation and ease with which beam transport can be achieved via optical fiber and robot manipulation. Heating of a thin surface layer takes place during a brief period of laser exposure, with thermal conduction into the work piece leading to rapid cooling and quenching [2]. The thickness of the hardened layer depends on the surface temperature and laser scanning velocity [3,4].

The principle barriers to widespread adoption of laser hardening in place of established technologies are tempering effects induced during multiple laser passes, where large areas must be treated, and residual stress evaluation for real mechanical components with complex geometry. The former may be overcome by using a rectangular laser spot that is wider than the surface to be treated [5] or by rapidly scanning the laser back and forth over the width of the work piece [6]; however, the required laser power increases with the width of the treated area, limiting the extent to which this technique can be exploited. Where multiple laser passes must nonetheless be performed, methods

have been presented for minimization of the softened zone [7]. The evaluation of residual stresses, on the other hand, requires case-by-case consideration due to the complexity of many real mechanical components. The stress state is the result of temperature gradients and microstructural changes during heating and cooling [8], with the extent of these effects strongly depend on the work piece geometry and the position of the treated area.

To date, a number of analytical and numerical models have been presented for evaluation of the temperature distribution during laser exposure of specific components for surface heat treatment [9,10]. Many authors have proposed evaluation criteria for prediction of phase changes based on temperature thresholds [11,12] and phase-change kinetic models [13,14,15]. Prediction of residual stresses has been performed for elementary components subject to simplified geometric constraints and a single laser pass [16,17,18] or alternate heating methods [19]. Experimental evaluation has also been performed for specific cases [20,21], including mechanical and fatigue-life assessment [22]. Despite these advances, there continues to be a lack of computational tools for the evaluation of residual stresses following laser surface hardening of arbitrary components; in particular, real mechanical components that by nature have complex geometry.

In light of this issue, together with the importance of structural integrity in real medium carbon steel parts subject to dynamic loading, the present work sees development of an efficient numerical model for assessment of the temperature distribution, phase changes and residual stresses during laser surface hardening of mechanical components with any geometry. Following on from earlier works dedicated

^{*} Corresponding author.

E-mail address: adrian.lutey2@unibo.it (A.H.A. Lutey).

to evaluation of temperature distributions and phase changes [7,23], residual stresses are calculated by determining deformation due to heating, cooling and microstructural changes [24]. The proposed model is verified against experimental results obtained for surface treatment of a medium carbon steel cam. Subsequently, the effects of laser fluence and scanning velocity are investigated theoretically by calculating changes in hardened depth and residual stress distribution for a number of different cases.

2. Process simulation

The process simulation is thermo-mechanical in nature, comprising models for evaluation of the temperature distribution, phase changes and residual stresses. Calculation of the time-dependent temperature field is first performed, based on the intensity of the incident laser beam and work piece properties such as thermal conductivity and optical absorptivity. The resulting microstructural changes due to the imposed thermal cycle are then determined based on phase-change thresholds and cooling rates. Finally, residual stresses are predicted according to the temperature distribution and microstructural changes in the treated area. The presented equations can be evaluated numerically for components with any geometry.

2.1. Thermal and microstructural models

Thermal and microstructural models are employed to evaluate the component temperature and resulting phases following laser exposure. A complete description of these models, including experimental validation, has been presented in previous works [7,23,25] and will be briefly summarized here within for reader convenience. The focused laser beam intensity is considered rectangular with a Gaussian top hat distribution:

$$I(x, y) = \frac{1}{4} \left[\operatorname{Erf} \left(\frac{A-2x}{2a\sqrt{2}} \right) + \operatorname{Erf} \left(\frac{A+2x}{2a\sqrt{2}} \right) \right] \cdot \left[\operatorname{Erf} \left(\frac{B-2y}{2b\sqrt{2}} \right) + \operatorname{Erf} \left(\frac{B+2y}{2b\sqrt{2}} \right) \right] \quad (1)$$

where A and B are the width and breadth of the intensity distribution and a and b define the rate of change in intensity at its edges. Such beam geometry was utilized to align with the characteristics of a diode laser used for experimental validation (Section 3). The quantity of energy delivered to the target is calculated based on the wavelength and temperature-dependent absorptivity of the target material. The thermal conductivity and specific heat capacity are considered temperature dependent in accordance with the literature [26].

These physical parameters are then utilized in Fourier's equation to resolve the time-dependent temperature distribution in the work piece during laser exposure:

$$\rho C_p \frac{\partial T}{\partial t} + Q = \nabla(k \nabla T) \quad (2)$$

where ρ is the density of the work piece in kg/m^3 , C_p is the heat capacity at constant pressure in $\text{J}/(\text{kg} \cdot \text{K})$, k is the thermal conductivity in $\text{W}/(\text{m} \cdot \text{K})$, Q the absorbed energy density in W/m^3 , T the temperature in K and t the time in s . Radiant heat losses from the work piece surface are not considered, while convective heat losses in air are taken into account with an ambient air temperature of 20°C .

Prediction of the resulting microstructural transformations is performed based on phase change threshold temperatures for both single and multiple laser passes. For single laser passes the only information necessary for process optimization is the maximum hardened depth and lateral extension, while for multiple laser passes, consideration of tempering effects is also necessary. The transformation constant for a

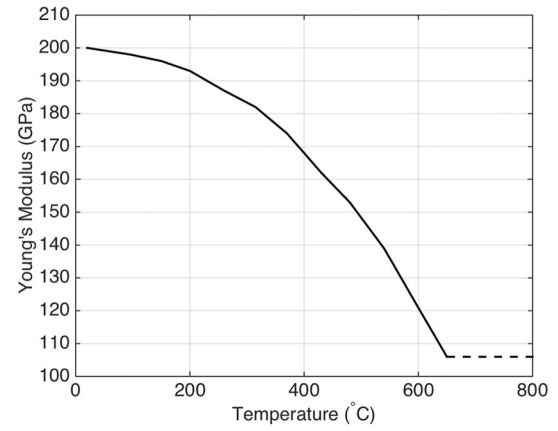


Fig. 1. Young's modulus as a function of temperature for medium carbon steel [29].

given phase change from phase i to phase j , $I_{i \rightarrow j}$, is calculated according to an Arrhenius-like equation introduced by Tani et al. [7,23]:

$$I_{i \rightarrow j} = \int_{t_{Ax}}^{t_{Ay}} \exp \left(-\frac{Q_{i \rightarrow j}}{RT(t)} \right) dt \quad (3)$$

where t_{Ax} and t_{Ay} are the start and finish times of the transformation, respectively, corresponding to the transformation start and finish temperatures, Ax and Ay . $Q_{i \rightarrow j}$ is the phase transformation activation energy and R is the universal gas constant.

2.2. Residual stress model

Exhaustive calculation of residual stresses is necessary for complete simulation of laser hardening for most mechanical applications; indeed, knowledge of this aspect plays a key role in selection of a particular heat treatment strategy. The residual stresses present in a component depend on its elasto-plastic behavior and are generated by both thermal expansion and microstructural changes [27]. The total deformation resulting from a given heating cycle, ε_{tot} , is:

$$\varepsilon_{tot} = \varepsilon^t + \varepsilon^{el} + \varepsilon^{pl} + \varepsilon^{tr} \quad (4)$$

where ε^t is the deformation due to thermal expansion, ε^{el} and ε^{pl} are the elastic and plastic deformations due to the thermal cycle and ε^{tr} is the contribution resulting from microstructural changes. In particular, the strain caused by thermal loading is calculated as follows:

$$\varepsilon^t = \alpha(T) \cdot (T(t) - T_0) \quad (5)$$

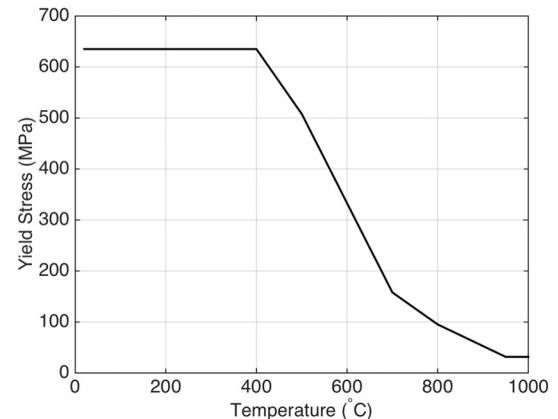


Fig. 2. Yield stress as a function of temperature [31].

Download English Version:

<https://daneshyari.com/en/article/8025179>

Download Persian Version:

<https://daneshyari.com/article/8025179>

[Daneshyari.com](https://daneshyari.com)